Available online at www.sciencedirect.com
ScienceDirect
Journal of Nuclear Materials 367–370 (2007) 173–178
journal of nuclear materials
www.elsevier.com/locate/jnucmat

Direct correlation between morphology of $(Fe,Cr)_{23}C_6$ precipitates and impact behavior of ODS steels

M. Klimiankou *, R. Lindau, A. Möslang

Institut für Materialforschung I, Forschungszentrum Karlsruhe GmbH, Postfach 3640, 76021 Karlsruhe, Germany

Abstract

The microstructure of ODS steels was investigated after different thermal and thermo-mechanical treatments by means of transmission electron microscopy (TEM) and analytical TEM techniques, including energy-dispersive X-ray (EDX) mapping of the elemental distribution at the nanometer scale. In 'as-HIPped' first generation ODS–Eurofer steel the grain boundaries were decorated with Cr-rich precipitates of $M_{23}C_6$ type. In addition, EDX mapping showed Cr-depleted areas at grain boundaries. Thermal and thermo-mechanical treatments of the ODS material affect the size, composition and spatial distribution of the precipitates. Depending on the treatments, the morphology and density of the $M_{23}C_6$ can be systematically varied. A significant decrease in ductile-to-brittle-transition-temperature (DBTT) in impact tests and an improvement in the tensile ductility at high temperature can be directly linked to the changes in precipitate morphology and size.

1. Introduction

Reduced-activation ferritic/martensitic (RAFM) steels were introduced in the international fusion materials programs about 20 years ago. The experience gained with fission reactor and accelerator facilities demonstrated attractive radiological properties, excellent thermal properties, and swelling resistance superior to austenitic steels [1]. In the past few years, oxide-dispersion-strengthened (ODS) steels produced by mechanical alloying techniques have become increasingly attractive for structural applications in nuclear fission and fusion power plants. The use of ODS alloys instead of the conventionally produced RAFM steels brings improved creep resistance at high temperatures and consequently allows an increase in the operating temperature of blanket structures in future fusion power reactors by 100 °C to approximately 650 °C or more [2,3]. Recently developed reduced-activation ferritic martensitic (RAFM) ODS steels based on the European RAFM reference steel Eurofer 97 [4] showed good tensile and creep properties, acceptable ductility, but poor impact behavior. These RAFM-ODS alloys were produced by PLANSEE using mechanical alloying of inert-gas-atomized RAFM Eurofer 97 steel powder [2,5] with addition of 0.3 wt% yttria powder in industrial attritor type ball mills. The approach was to fabricate near-net-shape blanket structures of first generation RAFM-ODS steel; using hot isostatic pressing (HIP) as the consolidation process (1150 °C,

* Corresponding author. Tel.: +49 7247 82 2903; fax: +49 7247 82 4567.
E-mail address: mikhail.klimiankou@imf.fzk.de (M. Klimiankou).

0022-3115/$ - see front matter
doi:10.1016/j.jnucmat.2007.03.150

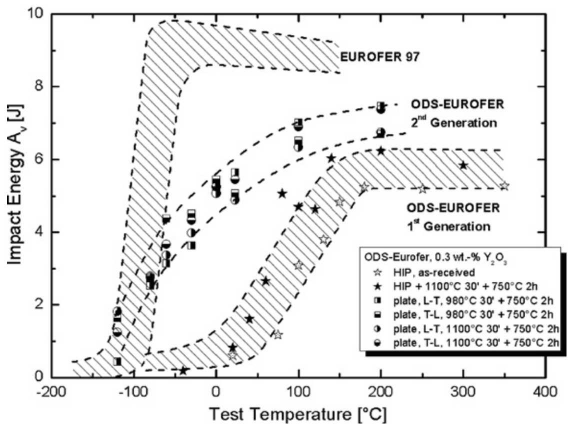

Fig. 1. Test temperature dependence of total absorbed energy of HIPped ODS–Eurofer (0.3 wt% Y_2O_3) and ODS–Eurofer plate material (0.3 wt% Y_2O_3) compared with RAFM steel Eurofer 97.

hold time 2 h, 100 MPa). More advanced blanket concepts like the helium cooled lithium lead (HCLL) blankets consist of a Eurofer 97 structure with SiC_f/SiC flow channel inserts in the self-cooled Pb–17Li breeding zone, which serve as thermal and electrical insulators, and a first wall which is plated with a 2–3 mm thick ODS-layer to withstand the high thermal and mechanical load [6]. A sheet of ODS–Eurofer steel ($6 \times 360 \times 730$ mm) was produced in cooperation between the Forschungszentrum Karlsruhe (FZK) and PLANSEE. The production route included compaction of the mechanically alloyed steel powder (0.3 wt% Y_2O_3) by HIP and subsequent hot rolling [5]. After an austenitisation and tempering treatment, the tensile ductility and impact behavior was significantly improved. The DBTT could be shifted from +60 to +100 °C for as-HIPped ODS–Eurofer of the 'first generation' to values between −40 and −80 °C, while the upper shelf energy was increased by about 40% (Fig. 1). Thereafter this thermo-mechanically treated material is called 'second generation' ODS–Eurofer steel.

2. Materials and methods

The ODS–Eurofer alloys examined in this study were either thermo-mechanically treated or HIPped and thermally treated under different conditions. The thermo-mechanical treatment includes hot rolling at 1150 °C + cooling to room temperature followed by re-austenitisation at 1100 °C for 30 min with water quenching and tempering at 750 °C for 2 h.

Three test series of ODS–Eurofer samples were treated in different ways. One batch was annealed for 2 h at 1000 °C, 1100 °C or 1200 °C. A second batch was additionally subjected to the standard re-austenitisation and tempering treatment (30 min at 1100 °C, water quenching + 2 h at 750 °C, air cooling). A third batch underwent a second HIPing under the same conditions as the first HIP. This treatment was introduced since it was observed that a second HIPping also improved the impact properties.

To gain insight into the origin of the differences in mechanical properties, extensive investigations of the microstructure dependence on the production and heat treatment parameters were performed. A FEI Tecnai 20 F transmission electron microscope (TEM) equipped with a field emission gun and operated at 200 kV accelerating voltage was used for the analytical work. The EDX experiments were performed in the scanning TEM (STEM) mode using a High angle annular dark field (HAADF) detector at a camera length of 100 mm for particle imaging. The EDX spectra were recorded using an EDAX Si/Li detector with ultra-thin window.

For the TEM examination disks of 0.15 mm thickness and 3 mm diameter were fabricated from the ODS materials by cutting, grinding and punching. TEM samples were prepared by electropolishing the disks in a TENUPOL 3 device at RT using a 20% H_2SO_4 + 80% methanol electrolyte, followed by three ultrasonic cleaning steps in ethanol.

3. Results and discussion

The TEM investigation of the microstructure of as-HIPped ODS–Eurofer of the first generation shows that the formation of $M_{23}C_6$ carbides at the boundaries of ferritic grains (Fig. 2) is a possible reason for the unfavorable DBTT and reduced upper shelf energy (USE). After HIPping and furnace cooling, this material has an equiaxed ferritic structure with a grain size varying from 2 μm to 8 μm. The scanning HAADF image of an $3 \times 5\ \mu m^2$ area containing several imaged grains is presented in Fig. 2(a). The precipitates on the grain boundaries are visible with a bright or dark contrast in the Fe (Fig. 2(b)) and Cr elemental maps (Fig. 2(c)). The quantitative evaluation of numerous EDX spectra from the precipitates show a Fe/Cr ratio of 0.85 ± 0.1. This high ratio is not typical for $M_{23}C_6$ precipitates in 9%Cr ferritic steels, where values of 0.30–0.37 were reported [7]. To exclude the

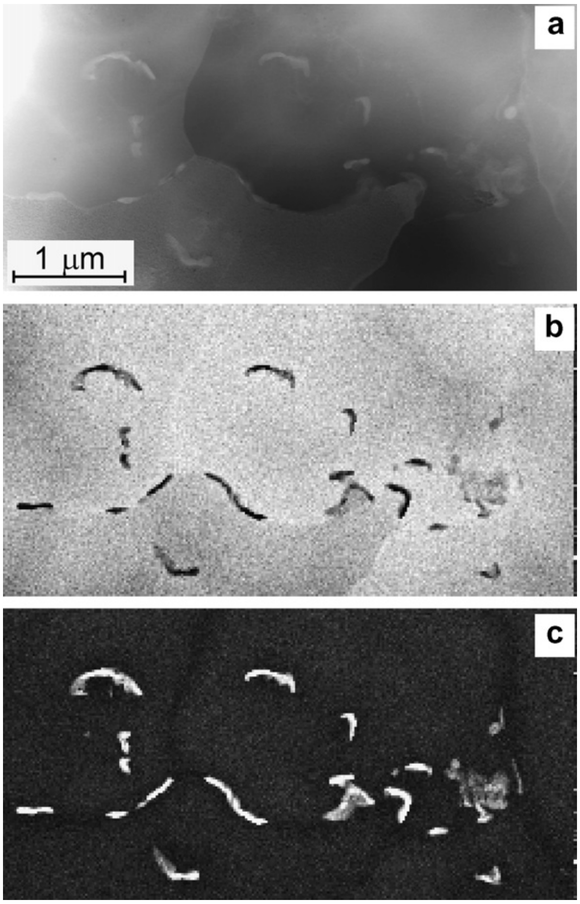

Fig. 2. STEM-HAADF image of a typical region with several ferritic grains in ODS–Eurofer (first generation) steel (a) (as-HIPped 1150 °C/2 h/100 MPa). The Fe- and Cr-distribution maps of the region are presented in Fig. 1(b) and (c), respectively.

influence of the surrounding Fe–matrix, the measurements were performed mainly at precipitates located close to the edge, where the sample thickness is less than 50 nm, which is well below the thickness of the precipitates (~80 nm). EELS investigations, that show the presence of carbon inside the precipitates, and HRTEM investigations of the structure lead to the conclusion that these long-shaped precipitates consist of $(Cr_{12}Fe_{10}W)C_6$ phase. The coverage degree of the grain boundaries was calculated as the ratio of the whole length to the covered length. The estimations show that 15–25% of the grain boundaries in the first generation ODS–Eurofer are covered with these precipitates. The EDX mapping also shows that grain boundaries are always visible with a slightly darker contrast in the Cr map and brighter in the Fe map (Fig. 2(b) and (c)). This effect is visible due to a 15–20% Cr depletion along the grain boundaries. The main consequences of the precipitation of $M_{23}C_6$ phase and Cr depletion are a significant degradation of tensile ductility [5], and impact properties (Fig. 1), as well as a reduced corrosion resistance.

The experimental observations that impact properties significantly improve after thermo-mechanical treatment lead to the search for the reasons in the microstructure. Several ODS–Eurofer samples with improved impact behaviour after thermo-mechanical treatment were characterized by TEM. The results show significant changes in both the structure of the grains/laths and morphology of $M_{23}C_6$ precipitates. In Fig. 3, for example, the results for a sample after hot rolling at 1150 °C followed by an austenitising and tempering (30 min at 1100 °C water quenching + 2 h at 750 °C air cooling) are presented. The HAADF image shows a decrease of the grain size to 0.6–2 μm (Fig. 3(a)). Martensitic grains, which are characterized by the lath structure

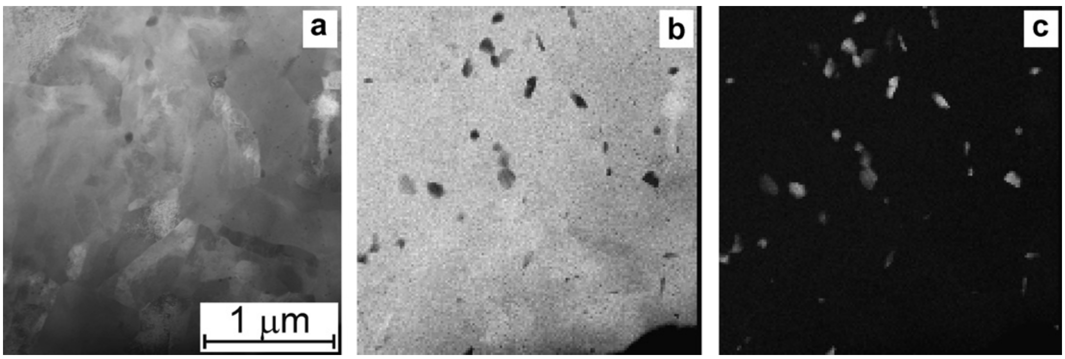

Fig. 3. STEM-HAADF image of a typical region in ODS–Eurofer steel (second generation) after thermo-mechanical treatment (a) (hot-rolled at 1150 °C + 30 min at 1100 °C + water quenching + 2 h at 750 °C + air cooling). The Fe- and Cr-distribution maps of the region are presented in Fig. 3(b) and (c), respectively.

and a high dislocation density, can be observed frequently. The $M_{23}C_6$ precipitates have a more globular shape and they are homogeneously distributed in the sample (Fig. 3(b) and (c)). The size of the precipitates varied from 50 nm to 400 nm. However, it can be estimated by statistical evaluation that about 20–30% of the precipitates locate directly on the prior austenitic grain (PAG) boundaries. In contrast to the only HIPped material, described above (Fig. 2), these grain boundaries do not show any detectable difference in the Cr concentration from the bulk (Fig. 3(c)). The Fe/Cr ratio of the precipitates ranges from 0.3 to 0.6 corresponding to an increase of the Cr concentration by factor 2.

When the same normalizing and tempering treatment (30 min at 1100 °C water quenching + 2 h at 750 °C air cooling) is applied to the ODS steel, given the second HIP treatment, the $M_{23}C_6$ precipitates can be detected again (Fig. 4). The investigations of the grain structure show that part of the material undergoes a martensitic transformation. In the HAADF image (Fig. 4(a)) an area with large grains that are free of defects is clearly visible. This area is marked in the image with a dashed line. The area marked with a dotted line in the lower left corner has a higher density of defects and exhibits a typical martensitic lath structure. The EDX mapping of the $3 \times 3\ \mu m^2$ area shows the re-formation of new numerous $M_{23}C_6$ precipitates with sizes of 30–100 nm. These precipitates can be clearly observed in the Fe and Cr maps as darker and brighter areas, respectively (Fig. 4(b) and (c)). The Fe/Cr ratio in these precipitates decreases, similar to the sample after thermo-mechanical treatment. These changes in the grain structure and distribution of $M_{23}C_6$ precipitates are similar to the one observed in the hot-rolled sample (Fig. 3). It can be suggested that the dissolution of long $M_{23}C_6$ precipitates which cover large areas of the grain boundaries and the formation of more homogenously distributed globular precipitates, as well as changes in the grain structure, are responsible for the changes of mechanical properties. The improvement of impact properties after thermal and thermo-mechanical treatment can be clearly seen in Fig. 1. Thermal treatment of the first generation ODS material leads to a small increase of the upper shelf energy (USE) and a shift of DBTT to a lower temperature in comparison to the HIPped material. Thermo-mechanical treatment, i.e., hot rolling plus thermal treatment causes a much greater improvement of USE and DBTT. This might be caused by the additional refinement of the grain size. Another contributing factor not yet proven is a possible densification of the material and/or breaking of presumably existing oxide films on the surface of the mechanically alloyed powders caused by the intensive working and deformation during the rolling procedure. An important result obtained by the TEM investigations is the formation of martensitic areas in both samples. These areas can be clearly identified based on their lath structure. The limited areas available for TEM investigations do not allow quantitative conclusions concerning the ratio of ferritic/martensitic areas, which were representative for the whole sample.

The different transformation behavior of ODS–Eurofer steel compared to Eurofer 97, which fully transforms to martensite even after air quenching, may have two main reasons. The first reason is, that

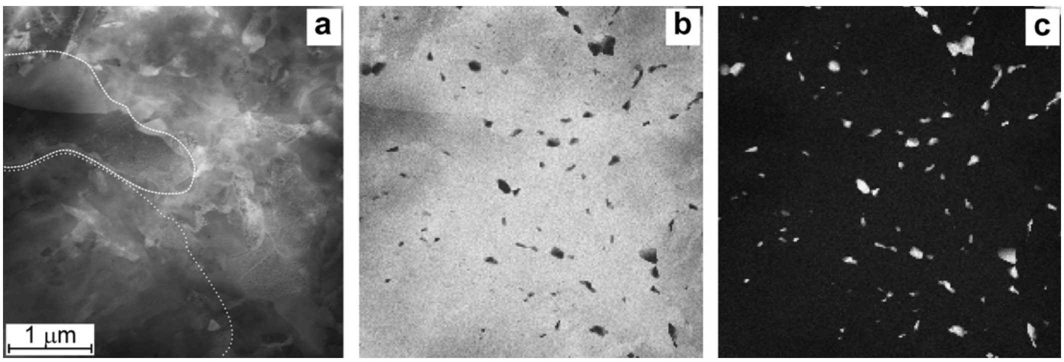

Fig. 4. STEM-HAADF image of a typical region in ODS–Eurofer steel (first generation), HIP 2 h at 1150 °C/100 MPa + 2 h at 1100 °C + water quenching with 2 h at 750 °C (a). The Fe- and Cr-distribution maps of the region are presented in Fig. 4(b) and (c) respectively.

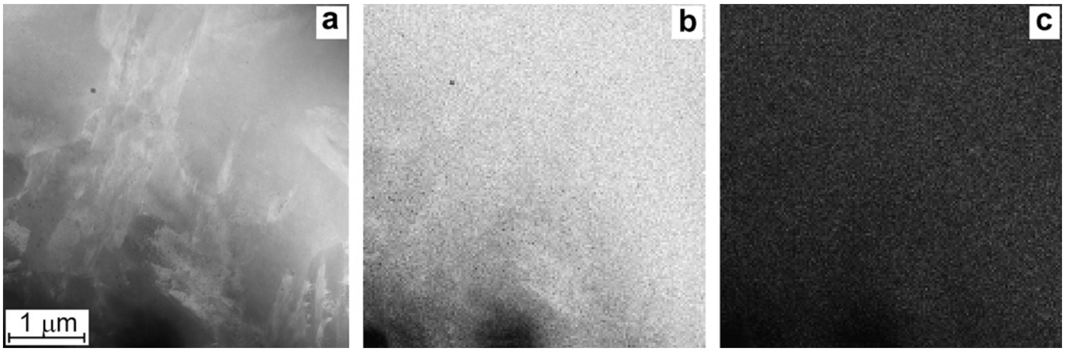

Fig. 5. STEM-HAADF image of a typical region in ODS–Eurofer steel (first generation) solution treatment (HIP 1150 °C/2 h/100 MPa + 2 h at 1100 °C + air cooling) (a). The Fe- and Cr-distribution maps of the region are presented in Fig. 5(b) and (c), respectively.

the carbon content decreased from 0.12 wt% in the Eurofer base material to 0.08 wt% in the Eurofer steel powder during the atomization process. Secondly, the very small sized grains provide enough nearby sinks for carbide precipitations.

Isochronal annealing experiments for 2 h at temperatures between 1000 and 1200 °C (air cooling) were performed to show whether or not it is possible to dissolve the massive carbide precipitations, which were observed after HIPping (Fig. 2). This showed that at 1100 °C and higher the $M_{23}C_6$ precipitates almost completely disappear (Fig. 5). The Fe (Fig. 5(b)) and Cr (Fig. 5(c)) EDX maps show homogeneous distribution of these elements. A careful searching with analytical EDX tool showed that $M_{23}C_6$ precipitates were still present in the sample, but with a density decreased by the factor 50–100. Due to the water cooling a martensitic grain structure of the sample was found. Annealing below 1100 °C results in the formation of martensitic areas free of any carbide precipitates, and ferritic areas. The boundaries between ferritic and martensitic areas are often decorated with small dispersed $M_{23}C_6$ precipitates. The long $M_{23}C_6$ precipitates still exist but the density is reduced by a factor of 2–5. The clear Cr depletion on the grain boundaries, detected in the ODS–Eurofer first generation, was not detected in this condition.

If solution annealed samples are treated with the standard normalizing and tempering treatment, globular $M_{23}C_6$ precipitates form again, comparable to those shown in Fig. 4.

A dissolution of $M_{23}C_6$ precipitates, similar to the sample annealed at 1100 °C (Fig. 5), can be achieved also by a second HIPping at 1300 °C. The sample treated at such high temperature additionally shows an increase of the average size of the ODS particles, which may lead to a degradation of tensile and creep properties. Samples HIPped at lower temperatures show a microstructure similar to the as-received condition (Fig. 2). The different dissolution behavior of the $M_{23}C_6$ precipitates in HIPped and annealed samples is caused by the retarded diffusion of C and Cr at the high pressure.

4. Conclusion

TEM investigations of ODS–Eurofer materials were conducted to determine the microstructural reasons for improved impact behavior caused by thermo- and thermo-mechanical treatment. We found that the dissolution of $M_{23}C_6$ precipitates covering the grain boundaries, the formation of ferritic–martensitic structures, and grain refinement are the main reasons for the improved of high temperature ductility and impact properties.

The TEM study shows the influence of thermal treatment conditions on the structure and distribution of $M_{23}C_6$ precipitates in ODS–Eurofer steel. The possibility of producing steels with tailored structures and thus controlled mechanical properties, was clearly demonstrated.

References

[1] K. Ehrlich, Philos. Trans. Roy. Soc. London Series A 357 (1999) 595.

[2] R. Lindau, A. Möslang, M. Schirra, P. Schlossmacher, M. Klimenkov, J. Nucl. Mater. 307–311 (2002) 769.

[3] S. Ukai, M. Fujiwara, J. Nucl. Mater. 307–311 (2002) 749.

[4] R. Lindau, A. Möslang, M. Rieth, M. Klimiankou, E. Materna-Morris, A. Alamo, A.A. F Tavassoli, C. Cayron, A.M. Lancha, P. Fernandez, N. Baluc, R. Schaublin, E.

Diegele, G. Filacchioni, J.W. Rensman, B. van der Schaaf, E. Lucon, W. Dietz, Fus. Eng. Des. 75–79 (2005) 989.
[5] R. Lindau, M. Klimiankou, A. Möslang, M. Rieth, B. Schedler, J. Schröder, A. Schwaiger, in: Proceedings 16th International Plansee Seminar, vol. 1, Reutte, Austria, 2005, p. 545.
[6] P. Norajitra, L. Bühler, U. Fischer, S. Gordeev, S. Malang, G. Reimann, Fus. Eng. Des. 69 (2003) 669.
[7] R.L. Klueh, D.R. Harries, High-Chromium Ferritic and Martensitic Steels for Nuclear Applications, West Conshohocken, PA, ASTM, 2001.